

**Antonio Soria-Verdugo<sup>1</sup>, Elke Goos<sup>2</sup>, Andrés Morato-Godino<sup>1</sup>, Nestor García-Hernando<sup>1</sup>, Uwe Riedel<sup>2</sup>,**  
***Pyrolysis of biofuels of the future: Sewage sludge and microalgae – Thermogravimetric analysis and***  
***modelling of the pyrolysis under different temperature conditions,***  
**Energy Conversion and Management, Volume 138, 15 April 2017, Pages 261–272.**

<sup>1</sup> **Carlos III University of Madrid (Spain), Energy Systems Engineering Group, Thermal and Fluids  
Engineering Department, Avda. de la Universidad 30, 28911 Leganés, Madrid, Spain**

<sup>2</sup> **Deutsches Zentrum für Luft- und Raumfahrt e.V. (DLR, German Aerospace Center), Institute of  
Combustion Technology, Pfaffenwaldring 38-40, 70569 Stuttgart, Germany**

The original publication is available at [www.elsevier.com](http://www.elsevier.com)

<https://doi.org/10.1016/j.enconman.2017.01.059>

## Pyrolysis of biofuels of the future: sewage sludge and microalgae -

### Thermogravimetric analysis and modelling of the pyrolysis under different temperature conditions

Antonio Soria-Verdugo<sup>a\*</sup>, Elke Goos<sup>b</sup>, Andrés Morato-Godino<sup>a</sup>, Nestor García-Hernando<sup>a</sup>, Uwe Riedel<sup>b</sup>

<sup>a</sup> *Carlos III University of Madrid (Spain), Energy Systems Engineering Group, Thermal and Fluids Engineering Department. Avda. de la Universidad 30, 28911 Leganés (Madrid, Spain).*

<sup>b</sup> *Deutsches Zentrum für Luft- und Raumfahrt e.V. (DLR, German Aerospace Center), Institute of Combustion Technology, Pfaffenwaldring 38-40, 70569 Stuttgart (Germany).*

\* *corresponding author: asoria@ing.uc3m.es Tel: +34916248465 Fax: +34916249430.*

#### Abstract

The pyrolysis process of microalgae and sewage sludge was investigated by means of non-isothermal thermogravimetric analysis. The Distributed Activation Energy Model (DAEM) was employed to obtain the pyrolysis kinetic parameters of the samples, i.e. the activation energy  $E_a$  and the pre-exponential factor  $k_0$ . Nine different pyrolysis tests at different constant heating rates were conducted in a thermogravimetric analyzer (TGA) to obtain accurate values of the pyrolysis kinetic parameters when applying DAEM. The accurate values of the activation energy and the pre-exponential factor that characterize the pyrolysis reaction of *Chlorella Vulgaris* and sewage sludge were reported, together with their associated uncertainties. The activation energy and pre-exponential factor for the *Chlorella Vulgaris* vary respectively between 150 - 250 kJ/mol and  $10^{10}$  -  $10^{15}$  s<sup>-1</sup>, whereas values ranging from 200 to 400 kJ/mol were obtained for the sewage sludge activation energy, and from  $10^{15}$  to  $10^{25}$  s<sup>-1</sup> for its pre-exponential factor. These values of  $E_a$  and  $k_0$  were employed to estimate the evolution of the reacted fraction with temperature during the pyrolysis of the samples under exponential and parabolic temperature increases, more typical for the pyrolysis reaction of fuel particles in industrial reactors. The estimations of the relation between the reacted fraction and the temperature for exponential and parabolic temperature increases were found to be in good agreement with the experimental values measured in the TGA for both the microalgae and the sludge samples. Therefore, the values reported in this work for the activation energy and the pre-exponential factor of the *Chlorella Vulgaris* can be employed as reference values in numerical studies of the pyrolysis process of this biofuel since its chemical composition is quite homogeneous. In the case of sewage sludge, due to the heterogeneity of its composition, the results reported for the kinetic parameters of the pyrolysis process can be employed to describe the pyrolysis of sludge with similar composition.

**Keywords:** Microalgae, Chlorella Vulgaris, Sewage Sludge, Distributed Activation Energy Model (DAEM), Biomass pyrolysis, Thermal Gravimetric Analysis (TGA).

**Nomenclature:**

- $a$  Heating rate [ $\text{K min}^{-1}$ ].
- $A_p$  Surface of a fuel particle [ $\text{m}^2$ ].
- $b$  Constant for the parabolic temperature profile [ $^{\circ}\text{C min}^{-2}$ ].
- $Bi$  Biot number [-].
- $c$  Constant for the exponential temperature profile [ $\text{min}^{-1}$ ].
- $c_p$  Specific heat of the fuel particle [ $\text{J kg K}^{-1}$ ].
- $E_a$  Activation energy [ $\text{kJ mol}^{-1}$ ].
- $f(E)$  Probability density function of the activation energy [-].
- $h$  Convective coefficient [ $\text{W m}^{-2} \text{K}^{-1}$ ].
- $k_f$  Fuel particle thermal conductivity [ $\text{W m}^{-1} \text{K}^{-1}$ ].
- $k_0$  Pre-exponential factor [ $\text{s}^{-1}$ ].
- $R$  Universal gas constant [ $\text{J mol}^{-1}\text{K}^{-1}$ ].
- $t$  Time [s].
- $T$  Temperature [ $^{\circ}\text{C}$ ].
- $T_p$  Fuel particle temperature [ $^{\circ}\text{C}$ ].
- $T_0$  Initial temperature of the fuel particle [ $^{\circ}\text{C}$ ].
- $T_{\infty}$  Temperature of the surrounding of the fuel particle inside a reactor [ $^{\circ}\text{C}$ ].
- $V$  Volatile mass loss [%].
- $V^*$  Volatile mass content [%].
- $V/V^*$  Reacted fraction [%].
- $V_p$  Fuel particle volume [ $\text{m}^3$ ].
- $\phi$   $\phi$  function [-].
- $\rho_p$  Fuel particle density [ $\text{kg m}^{-3}$ ].

## 1. Introduction

A continuous growth of the world population has occurred during the last 50 years, resulting in an increase of the primary energy consumption. Currently, more than 80% of the total primary energy consumption is based on fossil fuels, which are responsible for more than 98% of the carbon dioxide emissions to the atmosphere, causing the current global warming problems [1]. Therefore, there is a need to evaluate the

potential of different alternative fuels capable of substituting fossil fuels, with lower associated pollutant emissions. Two of the most promising alternative fuels, due to entirely different reasons, are sewage sludge and microalgae.

Sewage sludge is the residue produced during the treatment of industrial or municipal wastewater. The main ways of the disposing of sewage sludge nowadays can be divided into three applications: landfill, agricultural use and incineration or thermochemical conversion [2]. Nevertheless, the European regulations try to limit the amount of sewage sludge employed for landfill. Concerning the agricultural use, sewage sludge contains organic matter, nitrogen, and phosphorus, making them suitable as a fertilizer. However, the sludge may also concentrate heavy metals and pathogens, which could cause significant environmental problems. In contrast, the thermochemical conversion of sewage sludge [3] presents several benefits, such as the possibility to recover energy [4], the reduction of the residue volume by 70% and the thermal destruction of pathogens [5]. Furthermore, the population growth in urban areas causes also the problem of an increase in the sewage sludge production. Therefore, the thermochemical conversion of sewage sludge with energy recovery might solve the issue of the increase in residues produced due to the population growth, contributing to a reduction of the dependence on fossil fuels.

Among the potential replacement for fossil fuels, biodiesel is gaining importance in applications such as transport, where other possible substitute fuels count on a limited applicability. The production of biodiesel has been based on different crops, causing social problems as the dilemma regarding the risk of diverting farmland or crops for biofuels production to the detriment of the food supply. The so-called third generation biofuel obtained from microalgae can deal with these social problems since microalgae can be cultivated in freshwater, marine seawater or even wastewater [6]. Microalgae have higher photosynthesis efficiency than energy crops based on terrestrial lignocellulosic biomass, which would help to reduce the concentration of CO<sub>2</sub> in the atmosphere at a faster rate [7]. Besides, microalgae are the fastest-growing photosynthesizing organisms, being able to complete an entire growing cycle every few days [1]. There is a large number of species of microalgae, among them the most widely grown is *Chlorella Vulgaris* [8].

In comparison to other thermochemical conversion processes, such as combustion or gasification, pyrolysis presents the advantage of producing mainly an easy to store and transport liquid product, in particular for those fuels characterized by high volatile matter and low fixed carbon content, like sewage sludge and microalgae [9]. Pyrolysis was found to be the optimal thermochemical process for sewage sludge by [10], due to its favorable energy balance, material recovery, and zero-waste conversion. Several methods have been employed in the literature to model the pyrolysis process of biomass, such as the single step model [11], the two parallel reaction model [12], the three pseudo-components model [13], the sectional approach

model [14], or the Distributed Activation Energy Model (DAEM) [15]. Miura [16] and Miura and Maki [17] proposed a simplification for DAEM to easily obtain the activation energy and the pre-exponential factor of a sample from different thermogravimetric analysis (TGA) tests. This simplified DAEM has been employed, achieving a proper agreement with experimental measurements, for a wide variety of samples, such as coal [18], charcoal [19], polymers [20], oil shale [21], medical waste [22], sewage sludge [23], microalgae [24, 25], and several different types of biomass [26, 27, 28, 29, 30, 31].

In this work, the pyrolysis of the *Chlorella Vulgaris* microalgae and sewage sludge are investigated separately, by means of non-isothermal thermogravimetric analysis. TGA tests of both biomasses under different constant heating rates were conducted and the experimental results were employed as input data to apply the Distributed Activation Energy Model. Nine different TGA curves were employed for both the *Chlorella Vulgaris* and the sewage sludge samples in order to obtain accurate values of pyrolysis kinetic parameters, i.e. the activation energy and the pre-exponential factor, of the samples when applying DAEM [32]. The accurate values of the kinetic parameters of the pyrolysis reactions of *Chlorella Vulgaris* and sewage sludge are reported together with their associated uncertainties. Finally, the values of the activation energy and pre-exponential factor of the samples were employed to simulate the evolution of the pyrolysis process of the biomasses under exponential and parabolic temperature increases, more typical of the pyrolysis process of fuel particles in industrial reactors. The comparison of the numerical results with experimental measurements carried out in the TGA resulted in an excellent agreement.

## 2. Mathematical model

The simplified Distributed Activation Energy Model was applied to obtain accurate values of the activation energy  $E_a$  and the pre-exponential factor  $k_0$  of *Chlorella Vulgaris* and sewage sludge kinetics of pyrolysis. The activation energy is the energy needed to activate the pyrolysis reactions and the pre-exponential factor expresses the empirical temperature dependence of the reaction rate coefficient  $k$  [33].

DAEM considers a complex fuel as a mixture of components, which decompose following first-order reactions. Thus, a large number of independent irreversible first-order reactions occur simultaneously with different associated activation energies. The reacted fraction  $V/V^*$  in a pyrolysis reaction can be determined as [16]:

$$1 - \frac{V}{V^*} = \int_0^\infty \exp\left(-k_0 \int_0^t e^{-E/RT} dt\right) f(E) \cdot dE . \quad (1)$$

where  $V$  is the volatile matter content released at time  $t$ ,  $V^*$  is the total volatile matter content of the sample,  $k_0$  is the pre-exponential factor corresponding to the activation energy  $E$ ,  $R$  is the universal gas constant,

and  $f(E)$  is the probability density function of the activation energy. The exponential term in Eq. (1) is the so-called  $\phi$  function:

$$\phi(E, T) = \exp\left(-k_0 \int_0^t e^{-E/RT} dt\right) \quad (2)$$

which is typically approximated by a step function at a value of the activation energy  $E = E_a$ , obtaining for the reacted fraction:

$$\frac{V}{V^*} = 1 - \int_{E_a}^{\infty} f(E) \cdot dE = \int_0^{E_a} f(E) \cdot dE \quad (3)$$

Miura [16] proposed a value for  $\phi(E_a, T) = 0.58$ , which has been employed for several different types of mineral carbon and biomass samples obtaining good agreement with experimental measurements. Approximating the integral in the  $\phi$  function, for a constant heating rate  $a$ , to:

$$\phi(E, T) = \exp\left(-\frac{k_0}{a} \int_0^T e^{-E/RT} dT\right) \approx \exp\left(-\frac{k_0 RT^2}{aE} e^{-E/RT}\right) \quad (4)$$

and using the value proposed by Miura [16] for  $\phi(E_a, T) = 0.58$ , the widely used Arrhenius equation for the pyrolysis of a sample under a constant heating rate  $a$  can be derived:

$$\ln\left(\frac{a}{T^2}\right) = \ln\left(\frac{k_0 R}{E_a}\right) + 0.6075 - \frac{E_a}{R} \frac{1}{T} \quad (5)$$

Based on this Arrhenius equation, Miura and Maki [17] proposed a method to determine the activation energy  $E_a$  and the pre-exponential factor  $k_0$  of a sample from TGA curves of the pyrolysis process obtained for different heating rates  $a$ .

### 3. Experimental Measurements

The pyrolysis tests were performed in a thermogravimetric analyzer TGA Q500 from TA Instruments. A nitrogen flowrate of 60 ml/min was supplied to the furnace to guarantee the existence of an inert atmosphere. The temperature profile programmed to the TGA consisted of two processes occurring in series, first a drying process of the sample at 105 °C and then the pyrolysis process taking place when increasing the temperature of the sample in the inert atmosphere up to 800 °C. For the pyrolysis tests conducted to determine the kinetic parameters of the pyrolysis, a constant heating rate was used, and for a more industrial application, a series of consecutive constant heating rates obtaining exponential or parabolic temperature increases, as described in [34], were employed. For the pyrolysis measurements at constant

heating rates, nine different tests were carried out, as proposed by Soria-Verdugo et al. [32], using heating rates of 10, 13, 16, 19, 22, 25, 30, 35, 40 K/min. These heating rates are low compared to industrial applications, nevertheless similar results were obtained by [31] when applying DAEM to TGA curves obtained at higher heating rates.

The sensitivity of the TGA mass measurement is 0.1  $\mu\text{g}$  and the weighing precision is  $\pm 0.01\%$ . The dynamic baseline drift during a heating process of an empty platinum pan from 50  $^{\circ}\text{C}$  to 1000  $^{\circ}\text{C}$  at 20 K/min is lower than 50  $\mu\text{g}$  with no baseline subtraction. The TGA temperature accuracy during an isothermal process is  $\pm 1$   $^{\circ}\text{C}$  and the temperature precision is  $\pm 0.1$   $^{\circ}\text{C}$ . A mass of  $10.0 \pm 0.5$  mg of the sample, sieved previously under 100  $\mu\text{m}$ , was employed in the pyrolysis measurements in the TGA to reduce heat transfer effects in the sample [26, 35]. Each pyrolysis test was conducted three times to guarantee the repeatability of the process (obtaining differences lower than 1 %), and a blank experiment was also run for each heating rate to exclude buoyancy effects.

The mono-cellular green microalgae *Chlorella Vulgaris* have a diameter of 4-10  $\mu\text{m}$  and a spherical form. They grow in flowing or standing fresh and brackish water and contain as dried samples around 50% of proteins and a high amount of a multitude of unsaturated fatty acids, such as alpha-linolenic acid and carotenoids, as lutein. Additionally, they contain minerals with iron, calcium, magnesium, zinc, potassium, manganese and sulfur. The *Chlorella Vulgaris* microalgae samples employed for the study were cultivated and dried by the company AlgaEnergy S.A. in 2016 in Madrid.

The sludge was obtained from the municipal sewage treatment plant of Loeches (Madrid, Spain) in February 2016. The sludge was taken after the pre-drying process in a fluidized bed in the sewage treatment plant. This sewage sludge sample is quite different to the one investigated earlier [23], which was obtained from the municipal sewage treatment plant of La China (Madrid, Spain) in 2012.

The samples of *Chlorella Vulgaris* and sewage sludge were characterized by proximate and elemental analyses. The proximate analysis was performed in the TGA Q500 from TA Instruments to determine the moisture, ash, volatile matter, and fixed carbon contents of the samples. The moisture content was characterized as the mass released by the sample at 105  $^{\circ}\text{C}$ . The ash content was determined as the percentage of mass remaining after a heating of the sample up to 550  $^{\circ}\text{C}$ , supplying the furnace with an oxygen flow rate of 60 ml/min using a heating rate of 10 K/min, and an isothermal process at 550  $^{\circ}\text{C}$  until the mass of the sample stabilized. The volatile matter content of the samples was measured as the percentage of mass released by the sample during a heating process at a heating rate of 10 K/min from 105  $^{\circ}\text{C}$  to 900  $^{\circ}\text{C}$  and an isothermal process at 900  $^{\circ}\text{C}$  in an inert atmosphere which was obtained introducing a flux of

60 ml/min of nitrogen in the furnace, until the mass of the sample stabilized. Finally, the fixed carbon content was obtained from the difference between these two procedures.

The elemental analysis of the sample was carried out in a LECO TruSpec CHN analyzer, where the carbon and hydrogen content of the sample are measured using an infrared absorption detector for the exhaust gases obtained from a complete combustion of the sample. The nitrogen content is determined conducting the exhaust gases through a thermal conductivity cell. The carbon and nitrogen contents are measured with a precision of  $\pm 0.5\%$ , while the precision of the measurement of the hydrogen content is  $\pm 1\%$ . Heating value tests of the samples were also conducted in an isoperibolic calorimeter Parr 6300 with an instrument precision of 0.10% relative standard deviation. Control limits were based on 99% confidence (3 sigma) values. The calorimeter has a temperature resolution of 0.0001 °C (data obtained from the manufacturer Parr Instruments).

#### 4. Results and Discussion

The results of the chemical, thermogravimetric and kinetic analysis of microalgae and sewage sludge as potential biofuels of the future are shown and discussed in the following sections.

##### 4.1. Physical and chemical properties of *Chlorella Vulgaris* and Sewage sludge

The results obtained from the proximate analysis, the ultimate analysis and the heating value tests of the microalgae *Chlorella Vulgaris* and sewage sludge samples are reported in Table 1.

Table 1: Results obtained from the characterization of the *Chlorella vulgaris* and the sewage sludge samples (d: dry basis, daf: dry ash free, \* obtained by difference).

<b>Proximate analysis</b>		
	<i>Chlorella vulgaris</i>	Sewage sludge
Volatile matter [% d]	76.26	57.11
Fixed carbon* [% d]	10.63	8.23
Ash [% d]	13.11	34.66
<b>Elemental analysis</b>		
	<i>Chlorella vulgaris</i>	Sewage sludge
C [% daf]	59.06	56.46
H [% daf]	8.81	7.91
N [% daf]	11.39	8.42
O* [% daf]	20.74	27.21
<b>High heating value</b>		
	<i>Chlorella vulgaris</i>	Sewage sludge
HHV [MJ/kg]	21.57	15.73

Table 1 shows that the volatile matter content of both the *Chlorella Vulgaris* and the sewage sludge is high, and therefore the pyrolysis study of these biofuels is justified. Concerning the elemental analysis, the carbon



and hydrogen contents of *Chlorella Vulgaris* are higher than those of sewage sludge samples, resulting therefore in a higher heating value for the microalgae sample. The nitrogen content of both samples is high, which indicates a high pollution level of NO<sub>x</sub> emission if direct combustion of these biomasses is selected as the thermochemical conversion method. Therefore, an appropriate NO<sub>x</sub> after-treatment system is necessary to satisfy EU emission regulations. Additionally, the ash content, especially in sewage sludge, needs to be considered as it influences the optimal operation and maintenance conditions of pyrolysis, gasification, and combustion systems for instance through the formation of slag, which affect the heat transfer to the wall [36]. Also ash compounds like heavy metals should not end up in the environment due to their negatively impact on health of humans, animals, plants and microorganism.

The composition of *Chlorella Vulgaris* samples from different sources, shown in Table 2, is quite homogeneous.

Table 2: Comparison of characterization results of *Chlorella Vulgaris* samples. B: basis of the measurement, M: Moisture, V: Volatile matter, A: Ash, FC: Fixed Carbon, C: Carbon, H: Hydrogen, N: Nitrogen, S: Sulfur, O: Oxygen, w: wet, d: dry, daf: dry ash free, \* obtained by difference.

Ref	Proximate Analysis					Elemental Analysis						Heating Value		Origin of algae
	B	M [%]	V [%]	A [%]	FC* [%]	B	C [%]	H [%]	N [%]	S [%]	O* [%]	HHV [MJ/kg]	LHV [MJ/kg]	
This work	d	---	76.26	13.11	10.63	daf	59.06	8.81	11.39	---	20.74	21.57	---	Algaenergy company (Spain).
[37]	d	---	74.59	9.02	16.39	daf	53.01	8.67	3.26	---	35.05	22.02	---	<i>Chlorella vulgaris</i> ESP-31 collected from a fish pond in southern Taiwan.
[38]	w	4.9	72.7	11.0	11.4	daf	47.1	6.78	10.3	0.72	35.1	17.9	16.5	A4F-Algae for Future, Pataias, Portugal.
[39]	d	---	73.4 ± 0.3	4.7 ± 0.1	21.9 ± 0.3	d	41.1 ± 1.0	6.4 ± 0.4	7.4 ± 0.2	---	40.5 ± 1.6	17.7 ± 1.0	---	CNR, Institute of Ecosystem Study, Sesto Fiorentino, Italy. Grown in BG-11 medium.
[39]	d	---	79.4 ± 0.3	2.5 ± 0.1	18.1 ± 0.3	d	46.3 ± 0.9	6.8 ± 0.3	6 ± 3	---	38 ± 4	20.23 ± 0.5	---	CNR, Institute of Ecosystem Study, Sesto Fiorentino, Italy. Grown in N starved medium.
[40]	w	4.4	75.2	11.4	9.0	w	44.7	6.5	7.6	1.4	24.0	19.3	---	Shandong Firstspirulina Biotech Co., Ltd. (Binzhou, Shandong, China).
[41]	w	4.4	67.2	15.9	12.5	w	42.8	6.5	6.7	1.0	43.3	---	---	Algaenergy company (Spain).
[42]	d	6.2	---	21.6	---	d	46.1	6.1	6.7	0.4	19.1	20.4	---	<i>Chlorella</i> species, supplied by Ingrepro B.V. (Netherland)
[43]	d	---	55.37	10.28	34.35	d	47.84	6.41	9.01	1.46	25.0	---	21.88	Jiangmen Yue Jian Biotechnologies Co. Ltd. (Guangdong, China).
[44]	w	6.26	76.13	11.50	6.11	daf	47.32	6.90	8.48	0.85	36.45	---	---	Spirulina Bio-Engineering Co. Ltd. (China).

As can be seen from Table 3, sewage sludge samples are quite heterogeneous. The reason is that sewage sludge is a complex mixture of water, organic compounds (such as carbohydrates, lipids, and proteins), microorganisms which can be pathogenic before they were destroyed through heating processes, and inorganic substances e.g. silicates and metal containing compounds, which are left over as ash after a high-temperature heating process. The composition of sewage sludge depends strongly on the origin of the wastewater, e.g. industrial, agricultural or rain water and the season, as well as the used pretreatment methods, such as aerobic, anaerobic, chemical or thermal stabilization, dewatering, thickening and drying processes [45]. This influences, for instance, the pyrolysis product distribution as shown by [2] for three samples of anaerobically digested sewage sludge obtained from three different urban wastewater treatment plants.

Table 3: Comparison of characterization results of sewage sludge samples. B: basis of the measurement, M: Moisture, V: Volatile matter, A: Ash, FC: Fixed Carbon, C: Carbon, H: Hydrogen, N: Nitrogen, S: Sulfur, O: Oxygen, w: wet, d: dry, daf: dry ash free, \* obtained by difference.

Ref.	Proximate Analysis					Elemental Analysis						Heating Value		Origin of sludge
	B	M [%]	V [%]	A [%]	FC* [%]	B	C [%]	H [%]	N [%]	S [%]	O* [%]	HHV [MJ/kg]	LHV [MJ/kg]	
This work	d	---	57.11	34.66	8.23	daf	56.46	7.91	8.42	---	27.21	15.73	---	Municipal sewage treatment plant of Loeches (Madrid, Spain)
[23]	w	5.98	58.97	25.64	9.41	daf	45.39	7.69	6.95	1.78	38.19	11.58	---	Municipal sewage treatment plant of La China (Madrid, Spain)
[46]	w	6.2	49.5	37.1	7.2	d	---	---	---	1.13	---	---	12.44	Digested sludge
[46]	w	7.0	58.4	26.7	7.9	d	---	---	---	0.60	---	---	15.32	Undigested sludge
[47]	w	6.2	58.9	15.9	19.0	daf	58.5	9.0	5.0	0.045	27.45	20.43	---	Sludge samples from France
[48]	w	7.65	51.66	35.02	5.67	daf	58.5	5.8	0.53	1.43	33.74	13.16	---	Digested and dry sewage sludge from Sydney Water (Australia)
[49]	d	---	42.6 ± 4.9	52.8 ± 5.7	4.6 ± 1.1	d	21.1 ± 3.2	3.4 ± 0.4	3.2 ± 0.6	1.1 ± 0.3	18.4 ± 2.2	9.9 ± 1.6	---	Municipal, hospital, and industrial wastewater treatment plants in Bangkok (Thailand)
[50]	---	---	---	---	---	daf	50.20	7.16	5.85	2.23	34.55	---	---	Anaerobically stabilized sewage sludge from Zürich (Switzerland)
[51]	w	7.3	63.1	22.5	7.1	w	38.0	5.1	6.9	1.2	19.0	---	---	Municipal sewage sludge from Shanghai (China)
[51]	w	5.7	54.1	34.2	6.0	w	34.9	4.8	4.5	1.1	14.8	---	---	Municipal sewage sludge from Shanghai (China)
[52]	d	---	64.7	32.0	---	d	32.3	4.9	5.3	0.57	24.9	13.12	---	Polish sewage sludge, stabilized by anaerobic digestion, dehydration and thermal drying
[52]	d	---	63.5	36.2	---	d	33.1	4.8	4.8	0.64	20.4	12.79	---	Polish sewage sludge, stabilized by anaerobic digestion, dehydration and thermal drying
[52]	d	---	64.58	36.0	---	d	28.9	4.4	4.1	1.1	20.2	12.24	---	Polish sewage sludge, stabilized

														by anaerobic digestion, dehydration and thermal drying
[53]	w	6	43	46	5	daf	42.10	6.48	6.55	3.75	41.13	---	---	Urban wastewater sludge
[54]	d	---	55.0	37.9	---	d	36.2	4.5	5.6	1.1	14.7	15.4	---	Anaerobic digested sludge from waste waters of large city
[54]	d	---	42.9	53.8	---	d	22.7	3.3	3.1	0.9	16.1	9.5	---	Anaerobic digested sludge from waste waters of large city
[55]	d	---	60.7	29.5	---	d	35.7	5.2	3.5	0.72	25.4	16.56	---	Anaerobic sewage sludge from Spanish municipal urban wastewater.
[56]	---	---	---	---	---	d	32.1	4.58	3.88	2.12	---	---	---	Sewage sludge from industrial wastewater
[56]	---	---	---	---	---	d	30.97	4.39	3.72	1.18	---	---	---	Sewage sludge from industrial wastewater
[57]	---	---	---	---	---	d	38.7	5.94	3.96	0.91	---	---	---	Sewage sludge from Alicante, Spain. (Plant Rincón de León) 20% industrial wastewater
[57]	---	---	---	---	---	d	35.3	5.27	5.41	0.81	---	---	---	Sewage sludge from Alicante, Spain. (Plant Rincón de León) 20% industrial wastewater
[58]	w	6.82	50.39	36.85	5.94	daf	51.70	6.83	9.82	0.89	30.76	---	---	Sludge from different chemical industries in China
[58]	w	8.70	59.50	22.23	9.57	daf	49.49	6.76	10.21	1.03	32.51	---	---	Sludge from different chemical industries in China

#### 4.2. Determination of the kinetic parameters of the pyrolysis

The pyrolysis tests using constant heating rates were conducted under a controlled atmosphere in the thermogravimetric analyzer. The procedure described by Soria-Verdugo et al. [32] was followed to obtain accurate values of the kinetic parameters of the pyrolysis, i.e. the activation energy  $E_a$  and the pre-exponential factor  $k_0$ . Following this procedure, tests using nine different heating rates ( $a = 10, 13, 16, 19, 22, 25, 30, 35, 40$  K/min) were performed. The evolution of the reacted fraction  $V/V^*$ , defined as the percentage of the total volatile matter released by the sample, with temperature  $T$  is shown in Figure 1 a) for the *Chlorella Vulgaris* and in Figure 1 b) for the sewage sludge sample, up to a temperature of 600°C. Under a constant nitrogen flow, carbonaceous compounds, measured as fixed carbon amount, volatilize between 500 - 700 °C and the ash melts at temperatures above around 800°C, which was not investigated in this study.

The pyrolysis of both samples occurred between 150 and 600 °C, nevertheless the evolution of the reacted fraction of sewage sludge with temperature is more progressive than that of the microalgae sample, for which the pyrolysis takes place faster for temperatures in the range 250 - 450 °C. Furthermore, the effect of the heating rate variation on the reacted fraction is higher for the *Chlorella Vulgaris* sample, obtaining a displacement of the curve to higher temperatures when increasing the heating rate, a typical result for non-

isothermal pyrolysis reactions [59, 60]. This effect is slighter for the sewage sludge, resulting in a collapse of the reacted fraction curves for the different heating rates in a narrow zone.

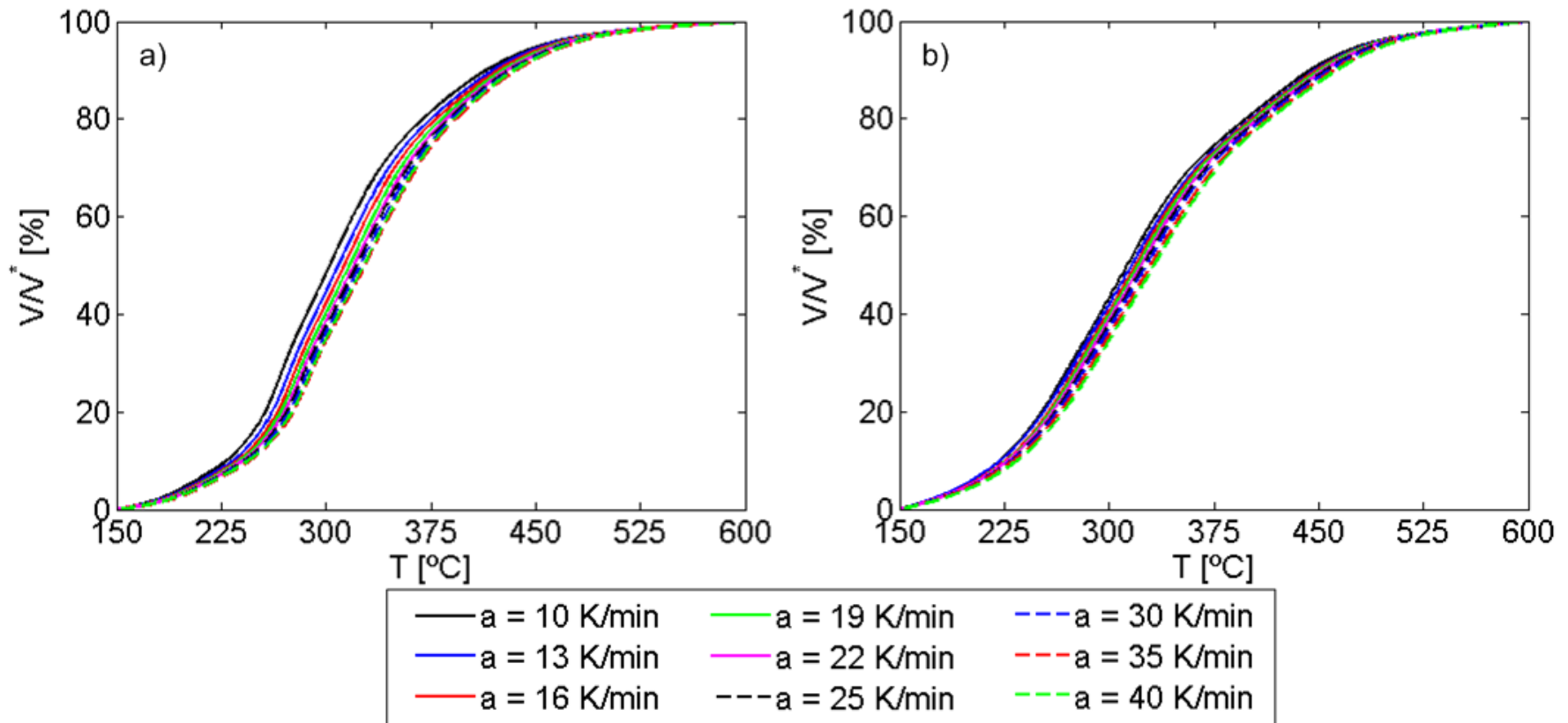


Figure 1: Evolution of the reacted fraction,  $V/V^*$ , with temperature,  $T$ , during the pyrolysis process at constant heating rates. a) *Chlorella Vulgaris*, b) Sewage sludge.

From the reacted fraction curves shown in Figure 1, and given the Arrhenius equation (Eq. 5), the Arrhenius plot can be built by plotting  $\ln(a/T^2)$  as a function of  $1/T$  for different values of the reacted fraction  $V/V^*$ . Figure 2 shows the Arrhenius plots of the *Chlorella Vulgaris* (a) and the sewage sludge (b). The Arrhenius plot of sewage sludge is wider because of the more progressive evolution of the reacted fraction with temperature observed in Figure 1 b). The Arrhenius plots can be employed to determine the activation energy  $E_a$  and the pre-exponential factor  $k_0$  of the samples by linearizing the points obtained for the different reacted fractions  $V/V^*$ . Both for the microalgae and the sludge samples, the points in the Arrhenius plot present a high linearity. To quantify the linearity of the Arrhenius plots, the determination coefficient of the linear fitting of the points,  $R^2$ , was calculated. The results can be observed in Figure 3, both for the *Chlorella Vulgaris* and the sewage sludge. A high linearity, i.e. high values of  $R^2$ , can be observed for a wide range of reacted fractions between 20% and 80%, whereas the values of the determination coefficient of the fitting decrease for low and high reacted fractions, where the slope of the curve  $V/V^*-T$  is smooth, as shown in Figure 1.

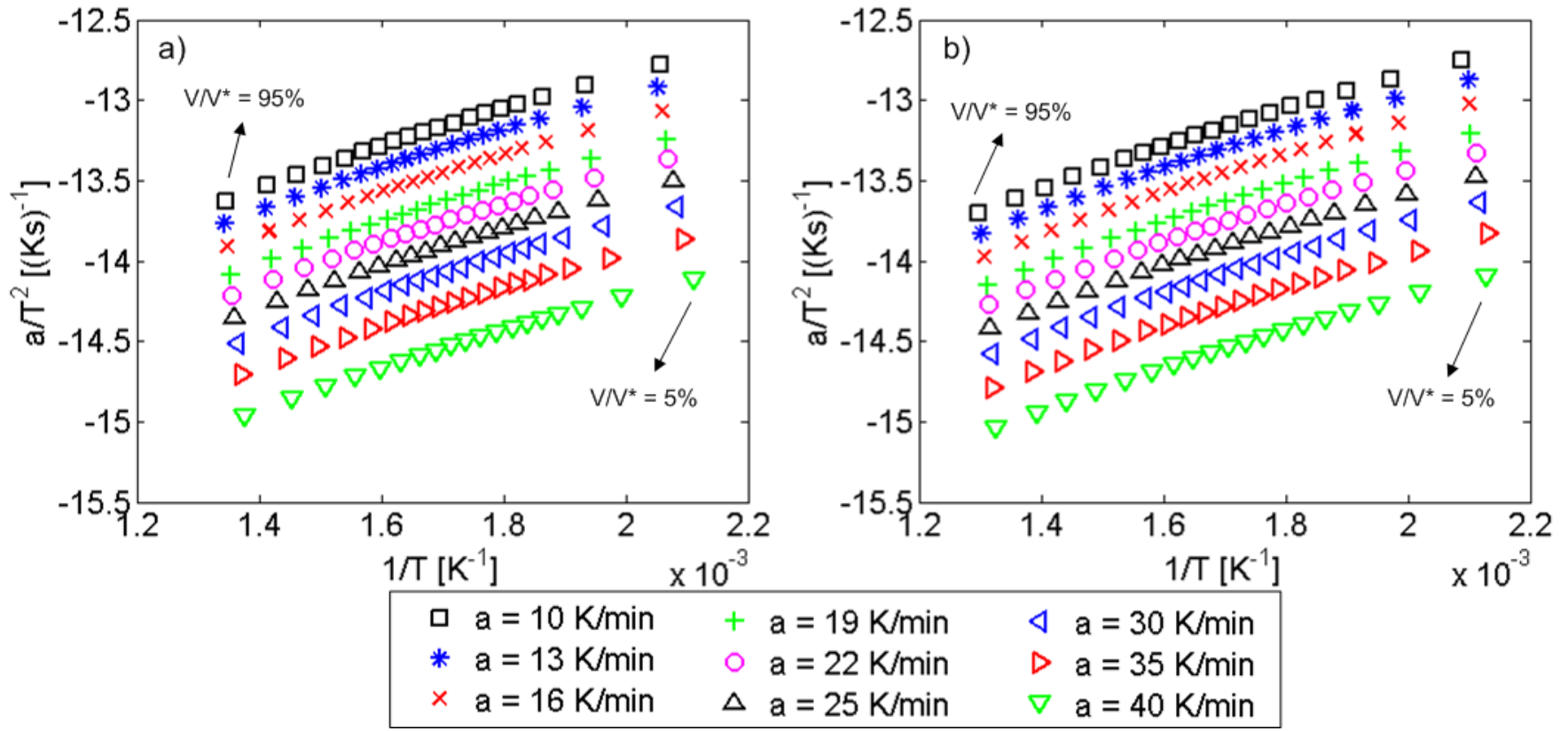


Figure 2: Arrhenius plot. a) *Chlorella Vulgaris*, b) Sewage sludge.

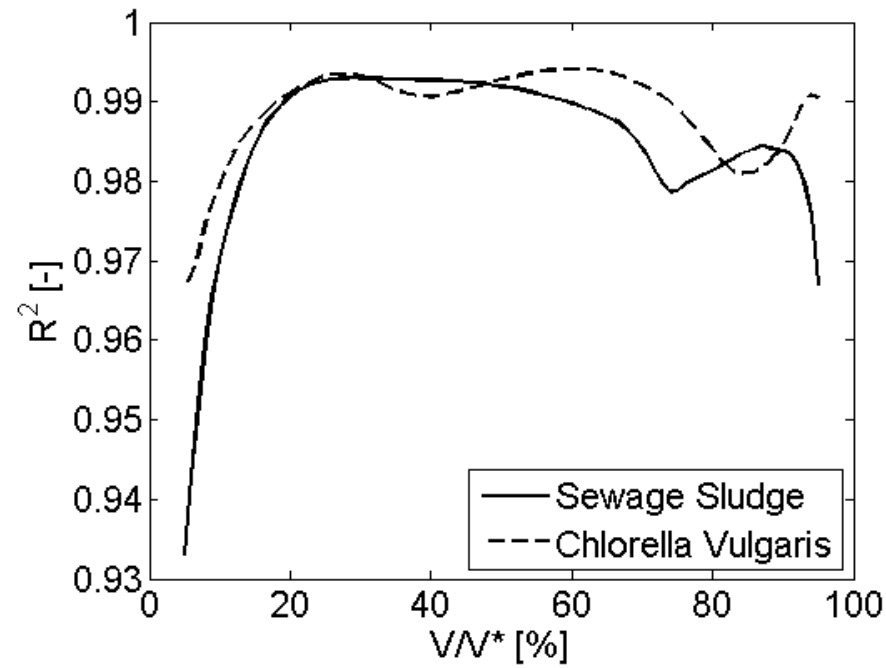


Figure 3: Determination coefficient of the linear fitting of the Arrhenius plot.

Considering the Arrhenius equation for constant heating rates (Eq. 5), the kinetic parameters of the pyrolysis reaction, i.e. the activation energy  $E_a$  and the pre-exponential factor  $k_0$ , can be obtained for each reacted fraction from the linear fitting of the values of the Arrhenius plot ( $\ln(a/T^2) = m \cdot (1/T) + n$ ). Equating terms of Eq. 5 with the linear fitting, the activation energy  $E_a$  and the pre-exponential factor  $k_0$  of the samples can be calculated from the slope  $m$  and the intercept  $n$  of the linear fitting as:

$$E_a = -m \cdot R \quad (6)$$

$$k_0 = -m \cdot \exp(n - 0.6075) \quad (7)$$

Accurate values of the activation energy  $E_a$  and the pre-exponential factor  $k_0$  can be calculated using the nine different reacted fraction curves shown in Figure 1, obtained for different constant heating rates, and

considering the uncertainties of the mass, the temperature  $T$  and the heating rate  $a$  for the linearization of the values of the Arrhenius plot, as stated by [32]. The accurate values of  $E_a$  and  $k_0$  for the *Chlorella Vulgaris* and the sewage sludge are shown in Figure 4. The activation energy of the *Chlorella Vulgaris* varies between around 150 and 250 kJ/mol, while its pre-exponential factor is in the range from  $10^{10}$  to  $10^{15}$  s<sup>-1</sup>. Similar values for the kinetic parameters of the pyrolysis reaction were obtained for *Chlorella microalgae* by [44, 38, 61-66], and for different microalgae such as *Nannochloropsis oculata* and *Tetraselmis sp.* by [24]. In contrast, higher values for both  $E_a$ , ranging from 200 and 400 kJ/mol, and  $k_0$ , varying between  $10^{15}$  and  $10^{25}$  s<sup>-1</sup>, were obtained for sewage sludge. These values of the kinetic parameters for sewage sludge are in accordance with the measurements of different authors [58,67-70]. In a previous work, [23] slightly lower values were obtained for the activation energy and pre-exponential factor of sewage sludge. Nonetheless, it should be noticed that the sewage sludge analyzed in [23] proceeded from the municipal sewage treatment plant of La China (Madrid, Spain) and were collected in 2012. Furthermore, the values of  $E_a$  and  $k_0$  reported in [23] were obtained from just three TGA curves and thus, a higher uncertainty could be expected for these values.

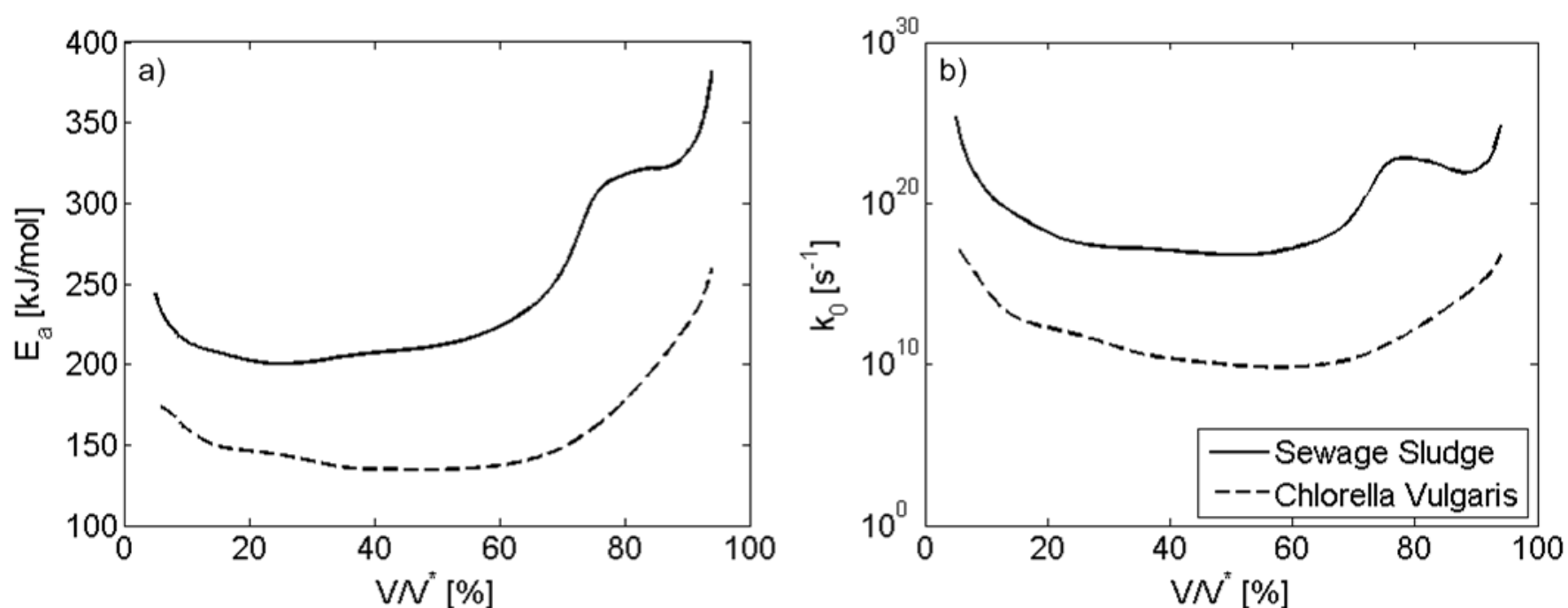


Figure 4: Kinetic parameters of the pyrolysis process: a) activation energy and b) pre-exponential factor.

The absolute and relative uncertainties associated with the kinetic parameters,  $E_a$  and  $k_0$ , of *Chlorella Vulgaris* and sewage sludge are reported in Figure 5. As can be observed, the absolute uncertainties of the activation energy depend on the stage of pyrolysis process and can be as low as 1.35 kJ/mol for the *Chlorella Vulgaris* algae and 2.03 kJ/mol for the sewage sludge, respectively. They are, for all the reacted fractions, lower than 2.5 kJ/mol for the *Chlorella Vulgaris*, and 4 kJ/mol for sewage sludge over the whole pyrolysis process, resulting in similar relative uncertainties of less than 1.3% for the activation energy of both samples. Nevertheless, the relative uncertainties for the pre-exponential factor differ, obtaining larger values for sewage sludge, as a result of its higher activation energy, shown in Figure 4 a), which means a higher

slope of the linearization that would lead to a higher uncertainty in the intercept of the linearization. For both the *Chlorella Vulgaris* and the sewage sludge, the relative uncertainty of the pre-exponential factor is higher for low and high values of the reacted fraction  $V/V^*$ , as a consequence of the lower linearity of the Arrhenius plot values in these zones, which can be proved by the lower determination coefficient  $R^2$  obtained for low and high  $V/V^*$  (Figure 3). Even though the values of the relative uncertainty of  $k_0$  might seem to be high, the effect of this parameter in the pyrolysis reaction is much lower than that of  $E_a$  due to the exponential function (see Eq. 1). Therefore, the values shown in Figure 4 for the activation energy and the pre-exponential factor of the *Chlorella Vulgaris* and the sewage sludge are accurate enough for most modelling and optimization purposes and could be employed to model the pyrolysis process of these types of biomass.

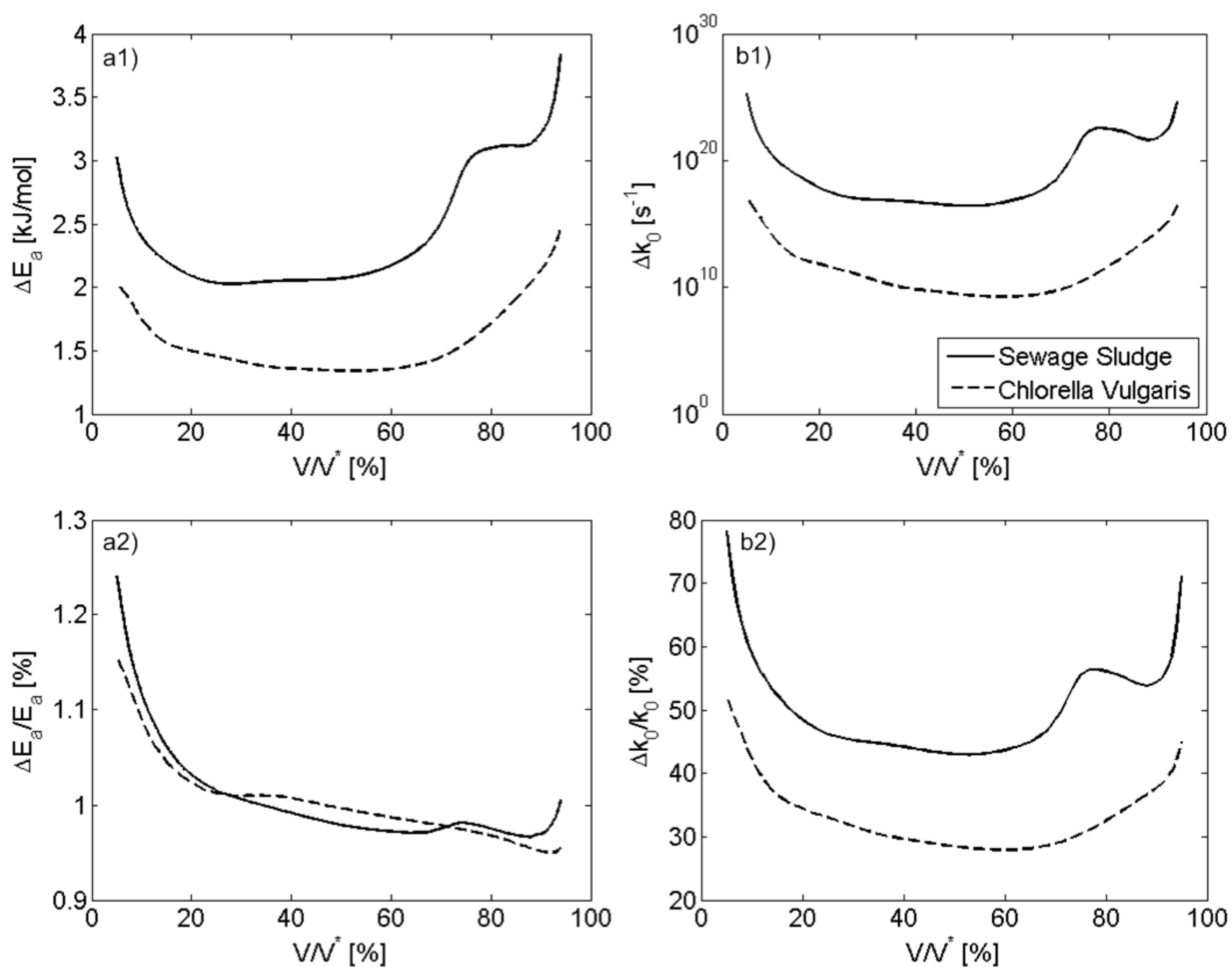


Figure 5: Uncertainties associated with the kinetic parameters of the pyrolysis process: a) activation energy, b) pre-exponential factor, 1) absolute uncertainty, 2) relative uncertainty.

#### 4.3. Validity of the kinetic parameters of pyrolysis for typical temperature increases of fuel particles

The values of the kinetic parameters of the pyrolysis process reported in Figure 4 and their associated uncertainties, shown in Figure 5, correspond to pulverized samples, with particles diameter below 100  $\mu m$ .

However, in industrial applications, the fuels to be pyrolysed are typically larger particles, such as pellets, and thus the temperature inside the fuel particles is subjected to heat transfer effects.

The evolution of the interior temperature of the fuel particles with time is governed by the Biot number,  $Bi$ , which relates the convective heat transfer between the solid surface and the surrounding with the heat transfer by conduction inside the particle. The Biot number is defined as:

$$Bi = \frac{h \cdot L_c}{k_f}, \quad (8)$$

where  $h$  is the convective coefficient,  $L_c$  is the characteristic length and  $k_f$  is the thermal conductivity of the fuel particle.

When the thermal conduction inside the fuel particle is much faster than the convective heat transfer at the particle surface, i.e.  $Bi \ll 1$ , the temperature variation inside the fuel particle can be neglected, assuming that the whole particle is at the surface temperature. In such cases, the Lumped Capacitance Method can be applied to determine the temperature variation inside the particle, equaling the energy increase inside the particle to the heat exchanged by convection on its surface. The result of the Lumped Capacitance Method is an exponential variation of the fuel particle temperature  $T_p(t)$  from its initial value  $T_0$  to the temperature of the environment inside the reactor  $T_\infty$ , in the form:

$$\frac{T_p(t) - T_\infty}{T_0 - T_\infty} = \exp\left[-\frac{h \cdot A_p}{\rho_p \cdot V_p \cdot c_p} t\right] \quad (9)$$

with the surface of a fuel particle  $A_p$ , the fuel particle density  $\rho_p$ , the fuel particle volume  $V_p$  and the specific heat of the fuel particle  $c_p$ .

In contrast, when the thermal conduction inside the fuel particle cannot be considered to be much faster than the convective heat transfer at the particle surface, the Lumped Capacitance Method is no longer valid, and the temperature inside the fuel particle differs from that of its surface. In these cases, the temperature distribution inside the fuel particle can be assumed to be parabolic.

Therefore, different tests were conducted in the TGA to characterize the pyrolysis of the *Chlorella Vulgaris* and the sewage sludge under exponential and parabolic temperature increases, following the trends of the temperature increases inside the fuel particles in industrial applications. Both the exponential and parabolic temperature increases were obtained in the TGA as a sequence of 25 short constant heating rate increases, as described in [33].



#### 4.4. Exponential temperature increases

The exponential temperature increases tested during the pyrolysis of the samples in the TGA were in the form:

$$T [^{\circ}\text{C}] = 146.5 + 3.5 \cdot \exp(c \cdot t). \quad (10)$$

Two different exponential temperature increases were programmed for each sample, varying the value of  $c$  ( $c = 0.023 \text{ min}^{-1}$  and  $c = 0.071 \text{ min}^{-1}$ ), these being the limit values studied in [34].

The Arrhenius equation derived from the simplified Distributed Activation Energy Model for exponential temperature increases was obtained by [34]:

$$\ln\left(\frac{c}{T}\right) = \ln\left(\frac{k_0 R}{E_a}\right) + 1.7467 - \frac{E_a}{R T}. \quad (11)$$

Therefore, Eq. 11 can be solved using the values of the activation energy  $E_a$  and the pre-exponential factor  $k_0$  of the sample, shown in Figure 4, to obtain the temperature  $T$  for each reacted fraction  $V/V^*$ . The results obtained solving Eq. 11 are presented in Figure 6 together with the experimental measurements of the pyrolysis process performed in the TGA under exponential temperature increases, for both the *Chlorella Vulgaris* and the sewage sludge samples. A proper agreement between the numerical results obtained from Eq. 11 and the experimental measurements can be observed in Figure 6 for both samples.

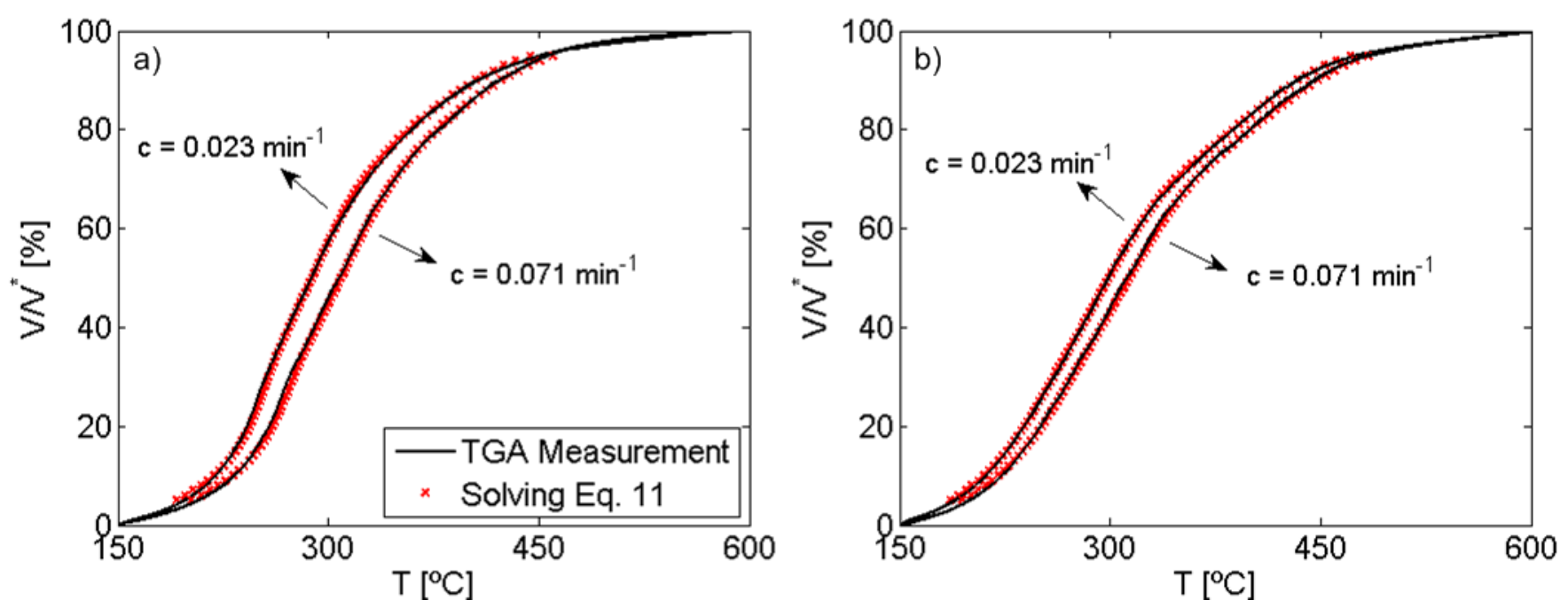


Figure 6: Comparison of experimental and numerical results obtained for the relation between the reacted fraction,  $V/V^*$ , and the temperature,  $T$ , during the pyrolysis process under exponential temperature increases. a) *Chlorella Vulgaris*, b) Sewage sludge.

The deviation between the numerical estimation of the temperature from Eq. 11 and the experimental measurement carried out in the TGA during the pyrolysis of the samples under exponential temperature

increases is shown in Figure 7 for total reaction times around 70 and 210 min, depending on the different exponential temperature profiles used. Low deviations of less than 4 °C between the numerically obtained and the experimentally measured temperature are obtained for both the microalgae and the sewage sludge samples for both exponential temperature profiles, in a range of reacted fractions between 20% and 80%, when the pyrolysis process is faster. Higher deviations of less than 9 °C are obtained for lower (<20%) and higher (>80%) values of the reacted fraction, where the linearity of the Arrhenius plot was lower (see Figure 3) and thus the uncertainties associated with the kinetic parameters of the pyrolysis reaction increased (see Figure 5). These low temperature deviations obtained for exponential temperature increases indicate that the activation energy  $E_a$  and the pre-exponential factor  $k_0$  shown in Figure 4 for the *Chlorella Vulgaris* and the sewage sludge pyrolysis, and the Arrhenius equation (Eq. 11) derived by Soria-Verdugo et al. [34], could be employed to simulate the pyrolysis process occurring in these fuel particles when the Lumped Capacitance Method can be applied.

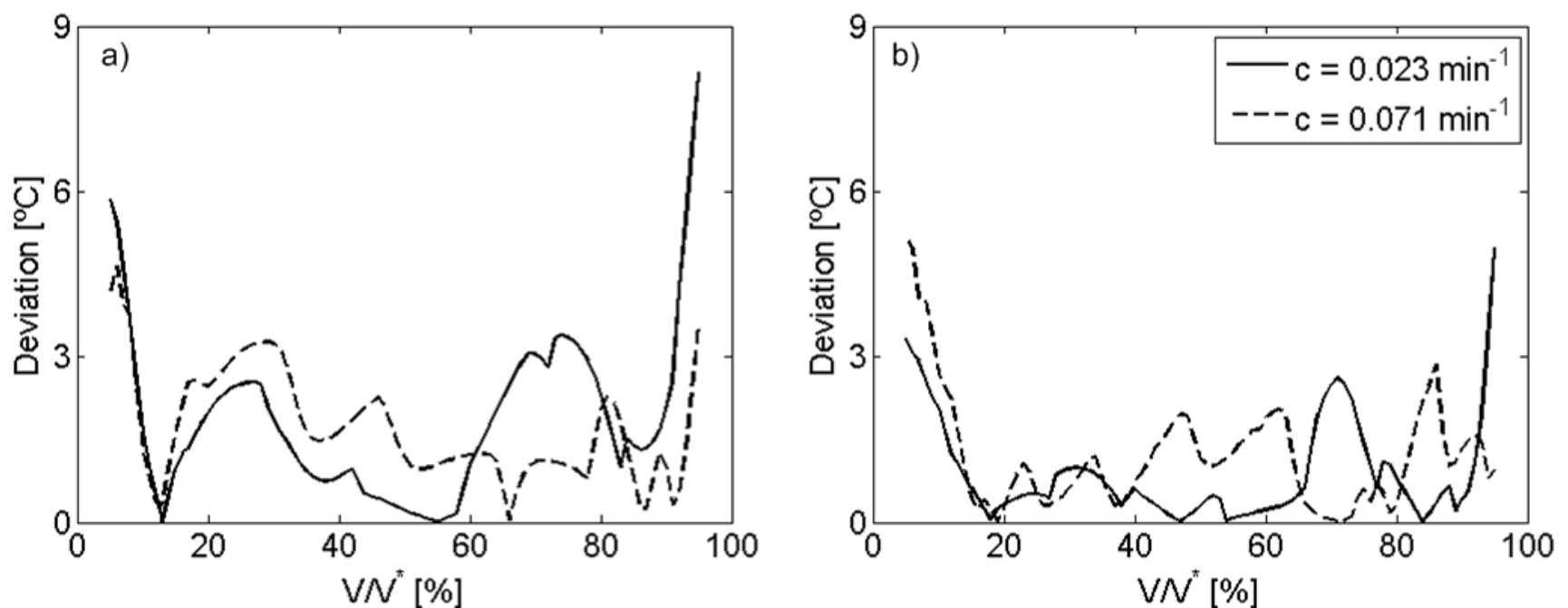


Figure 7: Deviations between the temperature estimated by the Arrhenius equation (Eq. 11) and the temperature measured in TGA for the pyrolysis under exponential temperature increases. a) *Chlorella Vulgaris*, b) Sewage sludge.

#### 4.5. Parabolic temperature increases

The parabolic temperature increases programmed in the TGA for the pyrolysis tests of the samples were in the form:

$$T[^\circ\text{C}] = 150 + b \cdot t^2 \quad (12)$$

Two different values of  $b$  ( $b = 0.050 \text{ }^\circ\text{C}\cdot\text{min}^{-2}$  and  $b = 0.464 \text{ }^\circ\text{C}\cdot\text{min}^{-2}$ ) were employed during the tests to obtain two different parabolic temperature increases during the pyrolysis measurements in the TGA, these being the limit values studied in [34].

Additionally, [34] obtained the Arrhenius equation derived from the simplified Distributed Activation Energy Model for parabolic temperature increases:

$$\ln\left(\frac{\sqrt{b}}{T^{1.5}}\right) = \ln\left(\frac{k_0 R}{2E_a}\right) + 1.0715 - \frac{E_a}{R} \frac{1}{T} \quad (13)$$

The values of the activation energy  $E_a$  and the pre-exponential factor  $k_0$  of the sample, shown in Figure 4, were used to solve Eq. 13, determining the temperature  $T$  at which each reacted fraction  $V/V^*$  occurred. The results of the measurements during the pyrolysis process of the samples in the TGA under parabolic temperature increases are plotted together with the numerical solution of Eq. 13 in Figure 8. A good agreement between the numerical estimation and the experimental measurements can be observed in Figure 8 both for the *Chlorella Vulgaris* and the sewage sludge pyrolysis processes. The pyrolysis processes with the lower value of  $b$  have a slower temperature rise with a more than 3 times longer reaction time (around 95 min for complete pyrolysis) which results in a higher amount of reacted fraction at lower temperature than during the pyrolysis processes with the higher value of  $b$ , which still needs more than 30 min for complete pyrolysis.

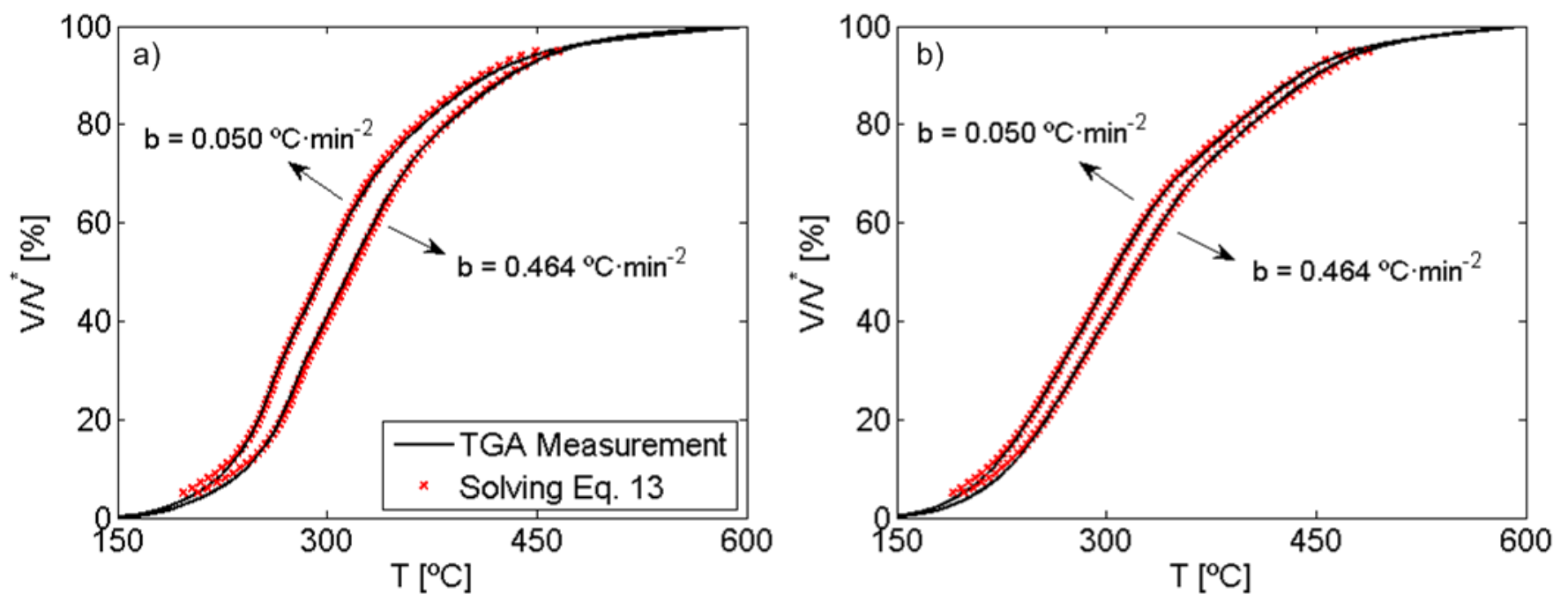


Figure 8: Comparison of experimental and numerical results obtained for the relation between the reacted fraction,  $V/V^*$ , and the temperature,  $T$ , during the pyrolysis process under parabolic temperature increases.

a) *Chlorella Vulgaris*, b) Sewage sludge.

The deviations between the temperatures estimated solving Eq. 13 and the TGA measurements during the pyrolysis process of the samples under parabolic temperature increases can be observed in Figure 9. The deviations between the numerical and the experimental temperature are again lower than 4 °C for a wide range of reacted fractions, between 20% and 80%. As for the case of the pyrolysis under exponential temperature increases, the temperature deviations for the pyrolysis under parabolic temperature increases

are slightly higher for reacted fractions lower than 20% and higher than 80%, where the uncertainties associated with the activation energy and the pre-exponential factor are higher (Figure 5). In view of the low deviations obtained between the numerical and the experimental temperatures, shown in Figure 9, the kinetic parameters of the pyrolysis reaction,  $E_a$  and  $k_0$ , for the *Chlorella Vulgaris* and the sewage sludge shown in Figure 4, and the Arrhenius equation (Eq. 13) derived by Soria-Verdugo et al. [34], could be employed to simulate the pyrolysis process occurring in these fuel particles subjected to parabolic temperature increases.

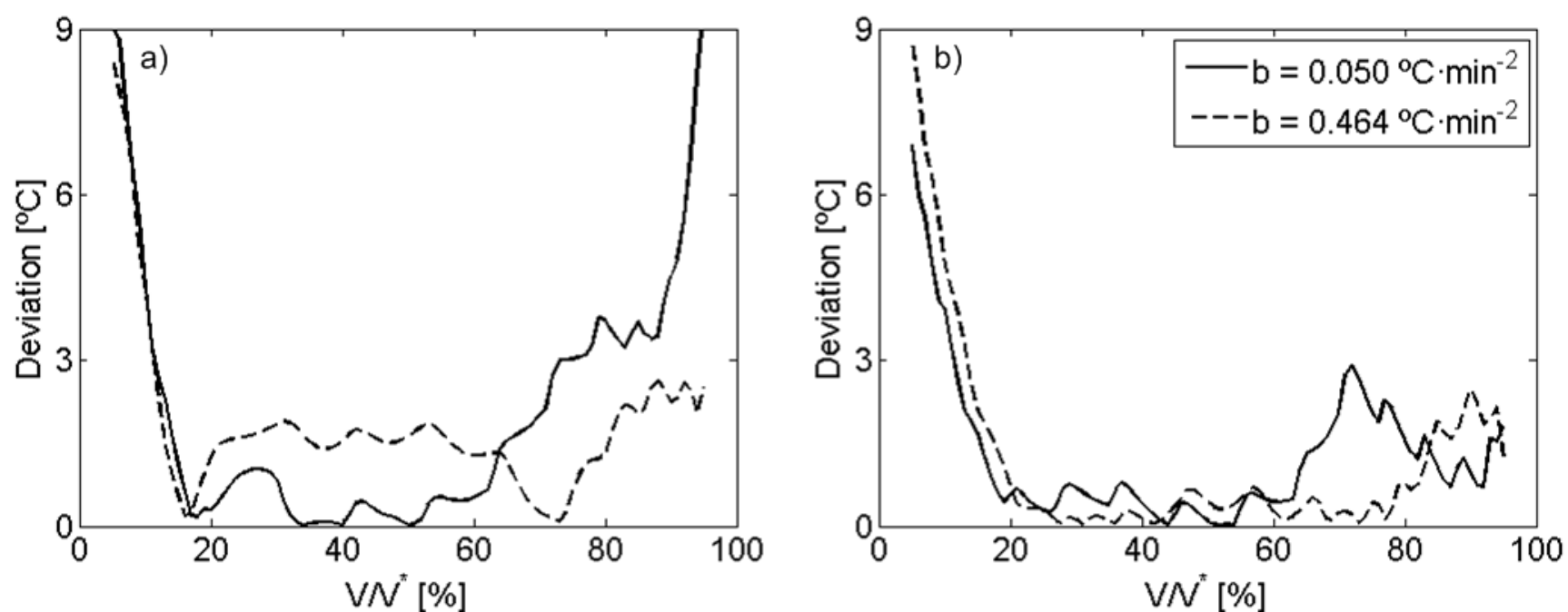


Figure 9: Deviations between the temperature estimated by the Arrhenius equation (Eq. 13) and the temperature measured in TGA for the pyrolysis under parabolic temperature increases. a) *Chlorella Vulgaris*, b) Sewage sludge.

## 5. Conclusions

The non-isothermal thermogravimetric analysis was employed to characterize the pyrolysis of *Chlorella Vulgaris* and sewage sludge. The simplified Distributed Activation Energy Model was applied to simulate the pyrolysis of the samples. Nine different TGA curves of the pyrolysis process of both samples, obtained for nine different constant heating rates, were used in the mathematical procedure described by the simplified DAEM to determine the kinetic parameters of the pyrolysis of the samples, the activation energy and the pre-exponential factor. The uncertainties associated with the temperature and mass measurements of the TGA and the constant heating rate were also considered in the mathematical calculation to reduce the uncertainties associated with the kinetic parameters of the samples.

The activation energies of *Chlorella Vulgaris* pyrolysis process are in the range of 150 – 250 kJ/mol and its pre-exponential factor varies between  $10^{10}$  and  $10^{15}$  s<sup>-1</sup> depending on the progress of the pyrolysis process. The values corresponding to the sewage sludge sample are slightly higher, with activation energies ranging

between 200 and 400 kJ/mol and pre-exponential factors from  $10^{15}$  to  $10^{20}$  s<sup>-1</sup>. The uncertainty associated to the activation energy of both samples is around 1%, whereas for the pre-exponential factor an uncertainty of around 30% was obtained for the *Chlorella Vulgaris* and around 50% for the sewage sludge pyrolysis process. Even though the uncertainties of the pre-exponential factor are much higher than those of the activation energy, their final effect on the calculation is limited since the pre-exponential factor is not included in the exponential function.

The validity of the obtained accurate values of the activation energy and pre-exponential factor of the *Chlorella Vulgaris* and the sewage sludge was evaluated for pyrolysis processes occurring under exponential and parabolic temperature increases, more typical of pyrolysis reactions of fuel particles in industrial applications. Experimental measurements of the pyrolysis process of the samples under exponential and parabolic temperature increases were conducted in the TGA, and the corresponding Arrhenius equations for these temperature increases were solved using the values obtained for the pyrolysis kinetic parameters. The comparison of the experimental and numerical data resulted in excellent agreement, confirming the accuracy of the values reported for  $E_a$  and  $k_0$ .

Therefore, the values reported for the activation energy and the pre-exponential factor for the *Chlorella Vulgaris* can be employed as reference values in numerical studies of the pyrolysis of this biofuel due to its homogeneity of chemical and biological composition, which is nearly independent of the place where these algae were cultivated. For sewage sludge pyrolysis the situation is quite different since its composition, especially the chemical composition, depends strongly on the source of the sewage sludge and differs significantly depending on the origin of the waste water used and its composition due to large differences between household, industrial, agricultural, and rain water. Therefore, the accurate pyrolysis kinetic values obtained for our sewage sludge sample can be used for modelling and optimizing sewage sludge pyrolysis processes with similar sewage sludge as feed stock, or in cases where no better data is available.

## **Acknowledgments**

The authors express their gratitude to the BIOLAB experimental facility and to the “Programa de movilidad de investigadores en centros de investigación extranjeros (Modalidad A)” from the Carlos III University of Madrid (Spain) for the financial support conceded to Antonio Soria for a research stay at the German Aerospace Center DLR (Stuttgart, Germany) during the summer of 2016. The authors also gratefully acknowledge the financial support provided by Fundación Iberdrola under the “VI Programa de Ayudas a la Investigación en Energía y Medioambiente”. Funding by the energy, combustion, and gas turbine technology program (EVG) of Deutsches Zentrum für Luft- und Raumfahrt e. V. (DLR), the German Aerospace Center,

is gratefully acknowledged as well as funding by the DLR international collaboration project "Accurate Kinetic Data of Biomass Pyrolysis".

## References

- [1] Demirbas A, Demirbas MF. Importance of algae oil as a source of biodiesel. *Energ. Convers. Manage.* 2011; 52, 163-170.
- [2] Fonts I, Azuara M, Gea G, Murillo MJB. Study of the pyrolysis liquids obtained from different sewage sludge. *J. Anal. Appl. Pyrol.* 2009; 85, 184-191.
- [3] Manara P, Zabaniotou A. Towards sewage sludge based biofuels via thermochemical conversion - A review. *Renew. Sust. Energ. Rev.* 2012; 16, 2566-2582.
- [4] Rulkens W. Sewage Sludge as a Biomass Resource for the Production of Energy: Overview and Assessment of the Various Options. *Energ. Fuel.* 2008; 22, 9–15.
- [5] Fytli D, Zabaniotou A, Utilization of sewage sludge in EU application of old and new methods - A review. *Renew. Sust. Energ. Rev.* 2008;12, 116–140.
- [6] Tran KQ, Bui HH, Chen WH. Distributed activation energy modelling for thermal decomposition of microalgae residues. *Chem. Eng. Transactions* 2016; 50, 175-180.
- [7] Milano J, Ong HC, Masjuki HH, Chong WT, Lam MK, Loh PK, Vellayan V. Microalgae biofuels as an alternative to fossil fuel for power generation. *Renew. Sust. Energ. Rev.* 2016; 58, 180-197.
- [8] Figueira CA, Moreira PF, Giudici R. Thermogravimetric analysis of the gasification of microalgae *Chlorella Vulgaris*. *Bioresource Technol.* 2015; 198, 717-724.
- [9] Marcilla A, Catalá L, García-Quesada JC, Valdés FJ, Hernández MR. A review of thermochemical conversion of microalgae. *Renew. Sust. Energ. Rev.* 2013; 27, 11-19.
- [10] Samolada MC, Zabaniotou AA. Comparative assessment of municipal sewage sludge incineration, gasification and pyrolysis for a sustainable sludge-to-energy management in Greece. *Waste Manag.* 2014; 34, 411-420.
- [11] Coats AW, Redfern JP. Kinetic parameters from thermogravimetric data. *Nature* 1964; 201, 68-69.
- [12] Anca-Couce A, Berger A, Zobel N. How to determine consistent biomass pyrolysis kinetics in a parallel reaction scheme. *Fuel* 2014; 123, 230-240.

- [13] Li Z, Zhao W, Meng B, Liu C, Zhu Q, Zhao G. Kinetic study of corn straw pyrolysis: comparison of two different three-pseudo component models. *Bioresource Technol.* 2008; 99, 7616–7622.
- [14] Lin T, Goos E, Riedel U. A sectional approach for biomass: Modelling the pyrolysis of cellulose. *Fuel Process. Technol.* 2013; 115, 246-253.
- [15] Vand V. A theory of the irreversible electrical resistance changes of metallic films evaporated in vacuum. *Proc. Phys. Soc.* 1943; 55, 222-246.
- [16] Miura K. A new and simple method to estimate  $f(E)$  and  $k_0(E)$  in the distributed activation energy model from three sets of experimental data. *Energ. Fuel.* 1995; 9, 302-307.
- [17] Miura K, Maki T. A simple method for estimating  $f(E)$  and  $k_0(E)$  in the distributed activation energy model. *Energ. Fuel.* 1998; 12, 864-869.
- [18] Günes M, Günes SK. Distributed activation energy model parameters of some Turkish coals. *Energy Sources Part A - Recovery Utilization and Environmental Effects* 2008; 30, 1460-1472.
- [19] Várghegyi G, Szabó P, Antal MJ. Kinetics of charcoal devolatilization. *Energ. Fuel.* 2002; 16, 724-731.
- [20] Wanjun T, Cunxin W, Donghua C. Kinetic studies on the pyrolysis of chitin and chitosan. *Polym. Degrad. Stabil.* 2005; 87, 389-394.
- [21] Wang Q, Wang H, Sun B, Bai J, Guan X. Interactions between oil shale and its semi-coke during co-combustion. *Fuel* 2009; 88, 1520-1529.
- [22] Yan JH, Zhu HM, Jiang XG, Chi Y, Cen KF. Analysis of volatile species kinetics during typical medical waste materials pyrolysis using a distributed activation energy model. *J. Hazard. Mater.* 2009; 162, 646-651.
- [23] Soria-Verdugo A, Garcia-Hernando N, Garcia-Gutierrez LM, Ruiz-Rivas U Analysis of biomass and sewage sludge devolatilization using the distributed activation energy model. *Energ. Convers. Manage.* 2013, 65, 239-244.
- [24] Ceylan S, Kazan D. Pyrolysis kinetics and thermal characteristics of microalgae *Nannochloropsis oculata* and *Tetraselmis* sp. *Bioresource Technol.* 2015; 187, 1-5.
- [25] Yang X, Zhang R, Fu J, Geng S, Cheng JJ, Sun Y. Pyrolysis kinetic and product analysis of different microalgal biomass by distributed activation energy model and pyrolysis-gas chromatography-mass spectrometry. *Bioresource Technol.* 2014; 163, 335-342.
- [26] Hu S, Jess A, Xu M. Kinetic study of Chinese biomass slow pyrolysis: Comparison of different kinetic models. *Fuel* 2007; 86, 2778-2788.

- [27] Cai J, Liu R. New distributed activation energy model: Numerical solution and application to pyrolysis kinetics of some types of biomass. *Bioresource Technol.* 2008; 99, 2795-2799.
- [28] Cai J, Wu W, Liu R. An overview of distributed activation energy model and its application in the pyrolysis of lignocellulosic biomass. *Renew. Sust. Energ. Rev.* 2014; 36, 236–246.
- [29] Sonobe T, Worasuwanarak N. Kinetic analyses of biomass pyrolysis using the distributed activation energy model. *Fuel* 2008; 87, 414-421.
- [30] Shen DK, Gu S, Jin B, Fang MX. Thermal degradation mechanisms of wood under inert and oxidative environments using DAEM methods. *Bioresource Technol.* 2011; 102, 2047-2052.
- [31] Soria-Verdugo A, Garcia-Gutierrez LM, Blanco-Cano L, Garcia-Gutierrez N, Ruiz-Rivas U. Evaluating the accuracy of the Distributed Activation Energy Model for biomass devolatilization curves obtained at high heating rates. *Energ. Convers. Manage.* 2014; 86 1045–1049.
- [32] Soria-Verdugo A, Goos E, Garcia-Hernando N. Effect of the number of TGA curves employed on the biomass pyrolysis kinetics results obtained using the Distributed Activation Energy Model. *Fuel Process. Technol.* 2015; 134, 360-371.
- [33] Soustelle M. *Handbook of heterogenous kinetics.* London: John Wiley & Sons; 2010.
- [34] Soria-Verdugo A, Goos E, Arrieta-Sanagustín J, García-Hernando N. Modeling of the pyrolysis of biomass under parabolic and exponential temperature increases using the Distributed Activation Energy Model. *Energ. Convers. Manage.* 2016; 118, 223-230.
- [35] Mani T, Murugan P, Abedi J, Mahinpey N. Pyrolysis of wheat straw in a thermogravimetric analyzer: effect of particle size and heating rate on devolatilization and estimation of global kinetics. *Chem. Eng. Res. Des.* 2010; 88, 952-958.
- [36] Vassilev SV, Vassileva CG. Composition, properties and challenges of algae biomass for biofuel application: An overview. *Fuel* 2016; 181, 1-33.
- [37] Bach QV, Chen WH, Lin SC, Sheen HK, Chang JS. Wet torrefaction of microalga *Chlorella Vulgaris* ESP-31 with microwave-assisted heating. *Energ. Convers. Manage.* 2016 [in Press]; <http://dx.doi.org/10.1016/j.enconman.2016.07.035>.
- [38] Ferreira AF, Soares Dias AP, Silva CM, Costa M. Evaluation of thermochemical properties of raw and extracted microalgae. *Energy* 2015; 92 365-372.



- [39] Belotti G, de Caprariis B, de Filippis P, Scarsella M, Verdone N. Effect of *Chlorella vulgaris* growing conditions on bio-oil production via fast pyrolysis. *Biomass Bioenerg.* 2014; 61, 187-195.
- [40] Gong X, Zhang B, Zhang Y, Huang Y, Xu M. Investigation on Pyrolysis of Low Lipid Microalgae *Chlorella Vulgaris* and *Dunaliella salina*. *Energ. Fuel.* 2014; 28, 95-103.
- [41] López-González D, Fernandez-Lopez M, Valverde JL, Sanchez-Silva L. Kinetic analysis and thermal characterization of the microalgae combustion process by thermal analysis coupled to mass spectrometry. *Appl. Energy* 2014; 114, 227-237.
- [42] Rizzo AM, Prussi M, Bettucci L, Libelli IM, Chiaramonti D. Characterization of microalga *Chlorella* as a fuel and its thermogravimetric behavior. *Appl. Energy* 2013; 102, 24-31.
- [43] Chen C, Lu Z, Ma X, Long J, Peng Y, Hu L, Lu Q. Oxy-fuel combustion characteristics and kinetics of microalgae *Chlorella Vulgaris* by thermogravimetric analysis. *Bioresour. Technol.* 2013; 144; 563–571.
- [44] Yuan T, Tahmasebi A, Yu J. Comparative study on pyrolysis of lignocellulosic and algal biomass using a thermogravimetric and a fixed-bed reactor. *Bioresour. Technol.* 2015; 175, 333-341.
- [45] Bresters AR, Coulomb I, Deak B, Matter B, Saabye A, Spinosa L, Utvik AØ, Uhre L, Meozzi P. Sludge Treatment and Disposal - Management Approaches and Experiences. Environmental Issues Series no. 7, 1-53, 1997 ISWA, European Environment Agency.
- [46] Scott SA, Dennis JS, Davidson JF, Hayhurst AN. Thermogravimetric measurements of the kinetics of pyrolysis of dried sewage sludge. *Fuel* 2006; 85, 1248–53.
- [47] Jayaraman K, Gökalp I. Pyrolysis, combustion and gasification characteristics of miscanthus and sewage sludge. *Energ. Convers. Manage.* 2015, 89, 83-91.
- [48] Kan T, Strezov V, Evans T. Effect of the Heating Rate on the Thermochemical Behavior and Biofuel Properties of Sewage Sludge Pyrolysis. *Energ. Fuel.* 2016; 30, 1564-1570.
- [49] Thipkhunthod P, Meeyoo V, Rangsunvigit P, Kitiyanan B, Siemanond K, Rirksomboon T. Pyrolytic characteristics of sewage sludge. *Chemosphere* 2006; 64, 955-962.
- [50] Dümpelmann R, Richarz W, Stammbach MR. Kinetic studies of the pyrolysis of sewage sludge by TGA and comparison with fluidized beds. *Can. J. Chem. Eng.* 1991; 69, 953.-963.
- [51] Fan H, He K. Fast Pyrolysis of Sewage Sludge in a Curie-Point Pyrolyzer: The Case of Sludge in the City of Shanghai, China. *Energ. Fuel.* 2016; 30, 1020-1026.

- [52] Magdziarz A, Werle S. Analysis of the combustion and pyrolysis of dried sewage sludge by TGA and MS. *Waste Manage.* 2014; 34, 174-179.
- [53] Jindarom C, Meeyoo V, Rirksomboon T, Rangsunvigit P. Thermochemical decomposition of sewage sludge in CO<sub>2</sub> and N<sub>2</sub> atmosphere. *Chemosphere* 2007; 67, 1477–1484.
- [54] Calvo LF, Otero M, Jenkins BM, García AI, Morán A. Heating process characteristics and kinetics of sewage sludge in different atmospheres. *Thermochim. Acta* 2004; 409; 127–135.
- [55] Inguanzo M, Domínguez A, Menéndez JA, Blanco CG, Pis JJ. On the pyrolysis of sewage sludge: the influence of pyrolysis conditions on solid, liquid and gas fractions. *J. Anal. Appl. Pyrol.* 2002; 63, 209-222.
- [56] Caballero JA, Front R, Marcilla A, Conesa JA. Characterization of sewage sludges by primary and secondary pyrolysis. *J. Anal. Appl. Pyrol.* 1997; 40-41, 433-450.
- [57] Conesa JA, Marcilla A, Prats D, Rodriguez-Pastor M. Kinetic study of the pyrolysis of sewage sludge. *Waste Manage. Res.* 1997; 15, 293-305.
- [58] Liu G, Song H, Wua J. Thermogravimetric study and kinetic analysis of dried industrial sludge pyrolysis. *Waste Manage.* 2015; 41, 128–133.
- [59] Munir S, Daood SS, Nimmo W, Cunliffe AM, Gibbs BM. Thermal analysis and devolatilization kinetics of cotton stalk, sugar cane bagasse and shea meal under nitrogen and air atmosphere, *Bioresource Technol.* 2009; 100, 1413-1418.
- [60] Tonbul Y, Saydut A, Yurdako K, Hamamci C. A kinetic investigation on the pyrolysis of Seguruk asphaltite. *J. Therm. Anal. Calorim.* 2009; 95, 197-202.
- [61] Chen C, Ma X, He Y. Co-pyrolysis characteristics of microalgae *Chlorella vulgaris* and coal through TGA. *Bioresource Technol.* 2012; 117, 264-273.
- [62] Maurya R, Ghosh T, Saravaia H, Paliwal C, Ghosh A, Mishra S. Non-isothermal pyrolysis of de-oiled microalgal biomass kinetics and evolved gas analysis. *Bioresour Technol* 2016;221:251–61.
- [63] Hu M, Chen Z, Guo D, Liu C, Xiao B, Hu Z, et al. Thermogravimetric study in pyrolysis kinetics of *Chlorella pyrenoidosa* and bloom-forming cyanobacteria. *Bioresour Technol* 2015;177:41–50.
- [64] Zhao B, Wang X, Yang X. Co-pyrolysis characteristics of microalgae *Isochrysis* and *Chlorella*: kinetics, biocrude yield and interaction. *Bioresour Technol* 2015;198:332–9.
- [65] Figueira CE, Moreira Jr PF, Giudicini R. Thermogravimetric analysis of the gasification of microalgae *Chlorella vulgaris*. *Bioresour Technol* 2015;198:717–24.

- [66] Kassim MA, Kirtania K, de la Cruz D, Cura N, Srivalsa SC, Bhattacharya S. Thermogravimetric analysis and kinetic characterization of lipid-extracted *Tetraselmis suecica* and *Chlorella* sp. *Algal Res* 2014;6:39–45.
- [67] Lin Y, Liao Y, Yu Z, Fang S, Lin Y, Fan Y, et al. Co-pyrolysis kinetics of sewage sludge and oil shale thermal decomposition using TGA-FTIR analysis. *Energy Convers Manage* 2016;118:345–52.
- [68] Huang L, Liu J, He Y, Sun S, Chen J, Sun J, et al. Thermodynamics and kinetics parameters of co-combustion between sewage sludge and water hyacinth in CO<sub>2</sub>/O<sub>2</sub> atmosphere as biomass to solid biofuel. *Bioresour Technol* 2016;218: 631–42.
- [69] Wang X, Zhao B, Yang X. Co-pyrolysis of microalgae and sewage sludge: biocrude assessment and char yield prediction. *Energy Convers Manage* 2016;117: 326–34.
- [70] Urych B, Smolinski A. Kinetics of sewage sludge pyrolysis and air gasification of its chars. *Energ. Fuel.* 2016; 30, 4869-4878.

## List of figures

Figure 1: Evolution of the reacted fraction,  $V/V^*$ , with temperature,  $T$ , during the pyrolysis process at constant heating rates. a) *Chlorella Vulgaris*, b) Sewage sludge.

Figure 2: Arrhenius plot. a) *Chlorella Vulgaris*, b) Sewage sludge.

Figure 3: Determination coefficient of the linear fitting of the Arrhenius plot.

Figure 4: Kinetic parameters of the pyrolysis process: a) activation energy and b) pre-exponential factor.

Figure 5: Uncertainties associated with the kinetic parameters of the pyrolysis process: a) activation energy, b) pre-exponential factor, 1) absolute uncertainty, 2) relative uncertainty.

Figure 6: Comparison of experimental and numerical results obtained for the relation between the reacted fraction,  $V/V^*$ , and the temperature,  $T$ , during the pyrolysis process under exponential temperature increases. a) *Chlorella Vulgaris*, b) Sewage sludge.

Figure 7: Deviations between the temperature estimated by the Arrhenius equation (Eq. 11) and the temperature measured in TGA for the pyrolysis under exponential temperature increases. a) *Chlorella Vulgaris*, b) Sewage sludge.

Figure 8: Comparison of experimental and numerical results obtained for the relation between the reacted fraction,  $V/V^*$ , and the temperature,  $T$ , during the pyrolysis process under parabolic temperature increases. a) *Chlorella Vulgaris*, b) Sewage sludge.

Figure 9: Deviations between the temperature estimated by the Arrhenius equation (Eq. 13) and the temperature measured in TGA for the pyrolysis under parabolic temperature increases. a) *Chlorella Vulgaris*, b) Sewage sludge.

## List of tables

Table 1: Results obtained from the characterization of the *Chlorella Vulgaris* and the sewage sludge samples (w: wet basis, daf: dry ash free basis, \* obtained by difference).

Table 2: Comparison of characterization results of *Chlorella Vulgaris* samples. M: Moisture, V: Volatile matter, A: Ash, FC: Fixed Carbon, C: Carbon, H: Hydrogen, N: Nitrogen, S: Sulfur, O: Oxygen, w: wet, d: dry, daf: dry ash free, \* obtained by difference.

Table 3: Comparison of characterization results of sewage sludge samples. M: Moisture, V: Volatile matter, A: Ash, FC: Fixed Carbon, C: Carbon, H: Hydrogen, N: Nitrogen, S: Sulfur, O: Oxygen, w: wet, d: dry, daf: dry ash free, \* obtained by difference.